

A DEEP LEARNING APPROACH USING VERY-HIGH SPATIAL RESOLUTION GAOFEN-2 IMAGES TO SUPPORT THE UNITED NATIONS SUSTAINABLE DEVELOPMENT GOAL INDICATOR 11.7.1 ASSESSMENT

Jiongbin Chen^{1,2}, Ping Zhang¹, Jun Zhang¹, Hao Wu^{1*}

¹ National Geomatics Center of China, Beijing 100830, China – (zhangping, junzhang, wuhao)@ngcc.cn

² College of Geoscience and Surveying Engineering, China University of Mining and Technology, Beijing 100083, China -
zqt2100205136@student.cumtb.edu.cn

KEY WORDS: Deep learning, Gaofen-2, Sustainable development goals, Urban green spaces, Accessibility analysis

ABSTRACT:

Since the proposal of the "2030 Agenda", the United Nations Sustainable Development Goal indicator 11.7.1 aims to calculate the accessibility and quality of urban open spaces(UOS). An accurate and rapid assessment framework of UOS is of great significance for urban sustainable development. Previous research on UOS has mainly focused on the evolution patterns of UOS, with little research on assessments of their accessibility for different population structures (i.e., men vs. women, young vs. older). In this study, a U-Net deep learning network was used for training from 3072 annotated samples of urban green spaces(UGS) which was created based on Gaofen-2 remote sensing images. The trained model was used to identify UGS within five districts of Beijing at sub-meter level, incorporated with Open Street Map and area of interest data. A spatial analysis was conducted for accessibility of UOS, finding that most of the UOS in the central urban area of Beijing can be reached within 10 minutes, but access to the eastern and western edges is poorer (more than 30 minutes). Finally, using Worldpop data, the accessibility of UOS was statistically analyzed for different ages and genders. The results show that UOS accessibility rate for the elderly and children reaches over 90% (10 minutes accessibility).

1. INTRODUCTION

In 2015, the United Nations 2030 Agenda for Sustainable Development (2030 Agenda) established 17 Sustainable Development Goals (SDGs) and 169 targets, with the aim of harmonizing the trinity of economic growth, social inclusion and environmental well-being (Colglazier, 2015). SDG 11.7.1 is "Average share of the built-up area of cities that is open space for public use for all, by sex, age and persons with disabilities". One important way to make cities more inclusive, safe and sustainable is to provide urban open spaces (UOS), which can provide many material and non-material benefits to residents through their environmental and social functions, and can improve the environmental quality of cities(Wai et al., 2018). In 2018, UN-HABITAT provided a technical paper describing the reference calculation steps and potential data sources for this SDG 11.7.1. And it suggests three steps: (1) Estimation of the land allocated to streets (LAS); (2) Estimation of the share of land allocated to

public open spaces; (3) Computation of core indicator: Average share of built-up area of cities that is open space for public use for all (UN-Habitat, 2018).

Previous research on UOS includes studying on the morphological changes of UOS under rapid urbanization (Zhu and Ling, 2022), the relationship between dynamic growth of UOS and walk ability (Liang et al., 2021), as well as landscape characteristics of UOS at different resolutions (Toger et al., 2015). The application of multiple methods has allowed for the identification of UOS in both temporal and spatial dimensions. Urban green spaces (UGS) such as parks and gardens, and urban squares as a type of urban grey space, are both important elements of UOS. It is worth noting that there are various definitions suited to different research needs. In this paper, it is argued that UOS serves as a place of recreation and entertainment for residents, and therefore encompasses both urban green spaces and urban squares.

Earth observation, especially using high-resolution

* Corresponding author

imagery, can help acquire more detailed urban information. Sub-meter satellite imagery not only accurately delineates land boundaries, but also reveals complex spatial relationships, facilitating the exploration of the interplay between economic growth, social activities, and environmental protection during the urban development process (Maso et al., 2020). Geospatial observation data can supplement or even replace inaccurate or invalid existing datasets (Verde et al., 2022). Earth observation plays a crucial role in advancing the implementation of the Sustainable Development Goals (SDGs) and the Global Indicator Framework, contributing to the tracking of progress in SDGs implementation, and providing indispensable information for SDGs planning and decision-making (Kavvada, 2020).

With the accumulation of increasingly abundant earth observation data, new applications of computer vision have been opened up, including but not limited to change detection, long-term monitoring, and image segmentation. The U-Net model is widely used for land-cover recognition due to its small data requirements, quick training process, and high accuracy in image segmentation. As a segmentation network algorithm evolved from fully convolutional network, U-Net neural network considers both global and detailed information of the image. Furthermore, U-Net concatenates the each layer of the encoder to the decoder, significantly enhancing the accuracy of the segmented image information and ultimately results (Ali et al., 2017; Abascal et al., 2022). Thus, the utilization of high-quality geospatial information and advanced deep learning techniques to obtain accurate UGS is critically significant for improved assessment of SDG 11.7.1 indicator.

Previous research on SDG 11.7.1 indicator mostly focus on calculating the proportion of area, but lacks spatial descriptions of urban open space that can serve residents. Accessibility analysis is the process of using destination point or area data and road data to conduct network analysis. By creating accessibility maps of a certain type of destination, it is possible to clearly reflect the spatial distribution of accessibility for that geographic feature. Accessibility analysis plays an important role in urban planning, assessing urban development potential, environmental protection, and enhancing residents' sense of well-being (Giuliani et al., 2021). Many scholars have used accessibility analysis to calculate SDG indicators, including infrastructure services, medical facility coverage, and resident education, supporting the calculations of SDG 1.4.1, SDG 3.8.1, and SDG 4.a.1, respectively. Building on existing research, accessibility analysis methods can be applied to UOS to calculate

their service range.

To address the urgent need for monitoring and measuring the Service scope of UOS, this paper developed an accurate and rapid assessment framework for the SDG 11.7.1 indicator assessment. This study introduces a deep learning U-Net framework that leverages earth observation advantages to extract UGS using sub-meter satellite images. 2) combine multiple-sources (i.e., area of interest, Open Street Map) acquired UOS 3) and explores the accessibility of services based on gender, age, especially for the elderly and children for supporting the assessment of SDG 11.7.1 indicator.

2. MATERIALS AND METHODS

2.1 Multiple sources of earth observation dataset

(1) *High-resolution Gaofen-2 images*. This study utilized high-resolution imagery from the Gaofen-2 satellite to cover 8 scenic areas in Beijing, China, with imaging dates ranging from 2020 to 2021. The areas covered include Dongcheng, Xicheng, Chaoyang, Haidian, and Shijingshan districts (Figure 1, (a)). The imagery has a resolution of 0.8 meters and was pre-processed with Digital Elevation Model data.

(2) *Multi-temporal Urban built-up area (UBA) datasets*. The study utilized data from the built-up areas of Beijing (Figure 1, (b)), delineated based on 30-m Global Artificial Impervious Surface data processed by Professor Gong Peng from Tsinghua University. This data was derived from high-resolution satellite imagery, which was used to identify impervious surfaces within urban areas (Shi et al., 2023). From 1900-2018, there are 7 years of urban boundary data available, and the 2018 data are used for this study.

(3) *Spatially-detailed population dataset*. The study utilized Worldpop population data for the year 2020 (Figure 1, (c)), with a spatial resolution of 100 meters(). A top-down, constrained approach was used to predict population counts, allowing for accurate depiction of residential areas and buildings and resulting in precise population distribution estimates. This approach also helped to reduce the impact of uninhabited areas on the analysis.

(4) *Multiple sources of Volunteered Geographic Information (VGI)*. The study utilized Open Street Map (OSM) road, Area of interest (AOI), and water body data (Figure 1, (d)). In the water information of OSM, there are three types of water-related areas: reservoir, riverbank, and water. These data are part of VGI and are characterized by its fast updates and diverse data

types. However, data gaps and accuracy issues are also common. After undergoing data quality checks and consistency checks, OSM data can be used to supplement urban open space ranges

and support the calculation of SDG 11.7.1 indicator. Additionally, The study utilized a sample set created from Google imagery to enhance training of the U-Net model(Shi et al., 2023).

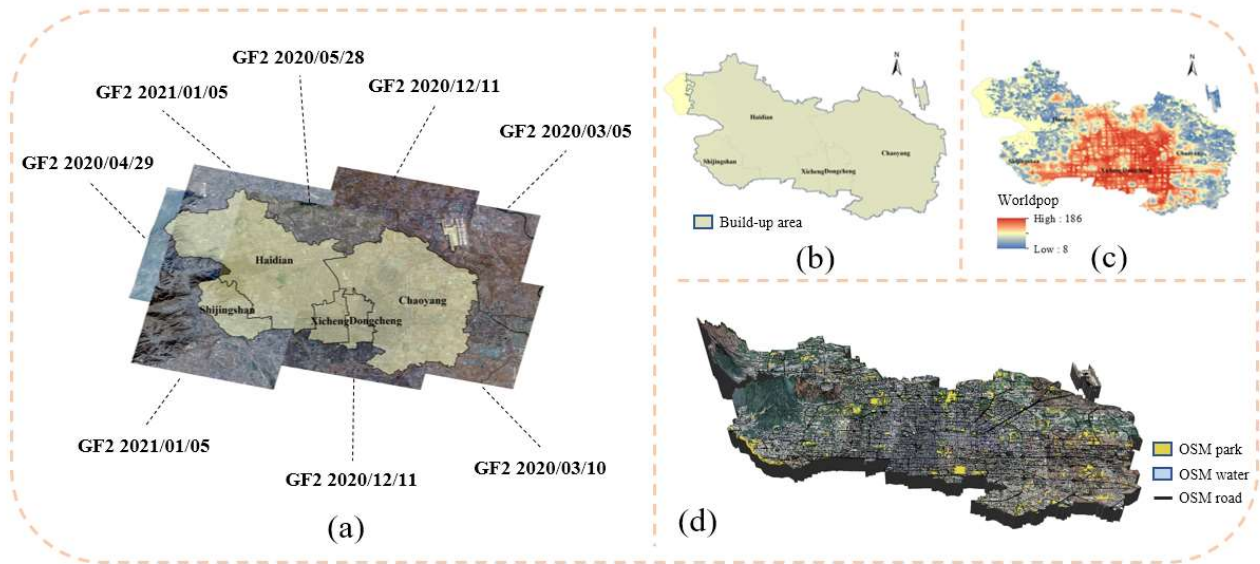


Figure 1. Research area and datasets: (a) date and location of Gaofen-2; (b) Urban built-up area; (c)Worldpop2020 data; (d)DEM and OSM data

2.2 Methods

High-resolution Gaofen-2 imagery was used in conjunction with the U-Net deep learning architecture to extract UGS. Then, Based on the identification results of UGS, combined with AOI data, the representation of UOS is carried out. Moreover, performing cost calculation on OSM road data, conducting accessibility analysis of UOS, and estimating the population within the service range.

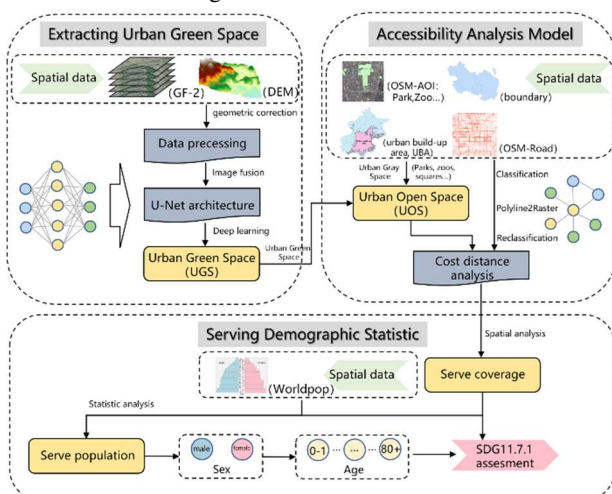


Figure 2. A framework of mapping UGS and supporting SDG 11.7.1 assessment derived multiple-source geo-spatial data

2.2.1 U-Net architecture

U-Net is a convolutional neural network proposed in 2015 for medical image segmentation, aiming to accurately locate and quantify objects within a specific category. Due to its excellent performance, it has been widely applied to various directions of semantic segmentation, such as satellite image segmentation (Ronneberger et al., 2015). U-Net is an Encoder-Decoder architecture, similar to fully convolutional network, where the front-end performs feature extraction and the back-end performs upsampling. The left half of the network comprises a downsampling module, consisting of two 3x3 convolutional layers with Rectified Linear Unit (ReLU) activation and a 2x2 max-pooling layer, designed to capture contextual features through convolutional operations. The right half of the network contains an upsampling module, including an upsampled convolutional layer, feature concatenation, and two 3x3 convolutional layers with ReLU activation, designed to localize the target object while incorporating corresponding features from the left-hand side.

The input to the left side of the network is a 512x512 image. Through paired 3x3 convolutions, the depth of the image is increased, followed by pooling operations to reduce the size of the image. At each downsampling step, the image is reduced by

half, while the number of convolutional filters is doubled. In the right side of the network, four upsampling steps are performed, resulting in an output of the same size as the original image. However, since deconvolution can only enlarge images rather than restore them, in order to reduce data loss, the approach is taken to crop the images from the left-hand side to the same size and concatenate them directly to the right-hand side to increase feature layers. Then, convolution is performed to extract features, and a 1x1 convolutional layer is used at the output layer to adjust the number of channels to match the number of object categories and obtain the segmentation result.

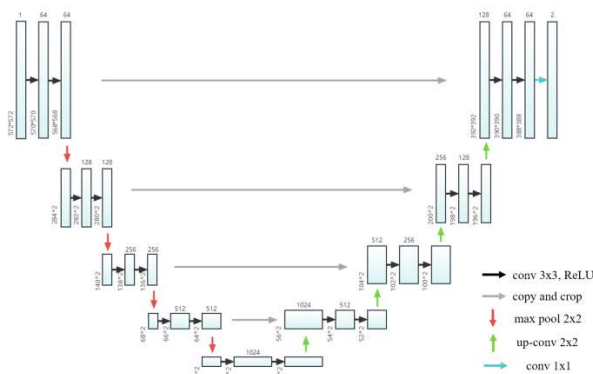


Figure 3. U-Net architecture (Ronneberger, 2015)

During the image segmentation process, it is necessary to segment objects of the same class that are in contact with each other. To better segment the boundaries of each object, weights need to be assigned to each pixel position during the training process to calculate the weighted loss. The weight of the boundary region is higher, which effectively strengthens the learning of boundary samples.

2.2.2 Service range analysis

Firstly, it is necessary to collect road data with different grades. The OSM road data has a class tag, which includes motorway, motorway link, trunk, trunk link, primary, primary link, secondary, secondary link, tertiary, and tertiary link types, corresponding to Chinese highways, first, second, and third level roads. Based on the design speed of Chinese highways and the actual situation of the research area, the speed for highways and expressways is determined to be 80 km/h, the speed for main roads is 60 km/h, the speed for secondary roads is 45 km/h, and the speed for urban roads is 35 km/h. Due to factors such as road conditions, weather, and traffic volume, the actual operating speed is often calculated by reducing the design speed and setting a reduction coefficient of 0.7. In addition, residents' travel modes

are often closely related to road length, and different travel distances lead to different probabilities of residents choosing walking or driving. Therefore, a designed driving probability is generated for determining the driving probability for each road (Table 1). Meanwhile, the walking speed on roads is set at 6 km/h, and off-road walking speed is set to 3.5 km/h. Finally, the time cost for one kilometer of road after revision is calculated.

Secondly, it is necessary to filter and clip other data in OSM. In the AOI surface data of OSM, there is a land use type named "park", which includes most parks and squares in Beijing and can be used as auxiliary information to determine UOS.

Distance(km)	Driving probability
$0 < d \leq 1$	$d/2$
$1 < d \leq 2$	0.5
$2 < d \leq 3$	$d/4$
$3 < d \leq 4$	0.75
$4 < d \leq 5$	$d/5$
$d > 5$	1

Table 1. Comparing Driving Probability on Roads

Thirdly, Accessibility analysis takes UOS, OSM water data, and OSM roads as input objects, and through analysis, the time from any location in the city to the nearest urban open space can be obtained. This involves analyzing the scale of UGS and squares and identifying service areas for developing green/grey open spaces (Pafi et al., 2016). Accessibility analysis typically includes two methods: the establishment of an Origin-Destination (OD) cost matrix for network analysis and gridded cost distance. The study use the gridded cost way to evaluate the accessibility of UOS within a geographic area for different population groups.

2.2.3 Accuracy Assessment

The Confusion Matrix serves as a fundamental tool in the evaluation of the predicted values with the Google Image Maps and UGS-1m(Shi et al., 2023). It is widely utilized to analyze and quantify the predictive accuracy and reliability of models in the field of image recognition.

	Predicted Positive	Predicted Negative
Actual Positive	TP	FN
Actual Negative	FP	TN

Table 2. Confusion Matrix

Where *TP* represents the number of instances that are actually predicted as positive, while *FN* indicates the instances

wrongly classified as negative. Conversely, *FP* refers to instances incorrectly classified as positive, and *TN* represents instances correctly classified as negative.

These metrics facilitate the computation of critical evaluation measures, including accuracy, precision, recall, and F1 score. These measures are essential in assessing the performance and effectiveness of classification models in the context of image recognition tasks.

$$Accuracy = \frac{(TP+TN)}{(TP+TN+FP+FN)} \quad (1)$$

$$Precision = \frac{TP}{(TP+FP)} \quad (2)$$

$$Recall = \frac{TP}{(TP+F)} \quad (3)$$

$$F1\ Score = 2 \times \frac{(Precision \times Recall)}{(Precision + Recall)} \quad (4)$$

A high accuracy represents that the model has a high percentage of correctly classified samples. A higher precision means that the model correctly identifies most of the actual positive cases, minimizing the chances of misdiagnosis and a higher recall rate means that the model is able to capture more true positive samples, reducing the risk of missing relevant positive samples (false negatives) by incorrectly predicting them as negative. A high F1 score means that the model is able to maintain a high level of precision while not sacrificing its ability to recognize positive samples.

3. RESULTS

3.1 Estimation of urban extent and the land allocated to

streets(LAS)

After applying Urban-Built-up Area(UBA) data filtering to exclude green space samples from non-urban areas, more accurate samples of UGS were obtained. Statistical analysis showed a area of 1,039.81 km² for the UBA across five in Beijing, accounting for 97% of the total area..

Following the method in section 2.2.2, road classification results were obtained as shown in Figure 4. The spatial extension of each road classification was performed according to Table 3, followed by resampling to the same resolution. The results found that total surface of urban streets to be 168.96 km² Then, estimating the official recommended metric LAS by eq(5):

$$LAS = \left[\frac{\text{Total surface of urban streets}}{\text{Total surface of urban area}} \right] \times 100\% \quad (5)$$

LAS refer to land allocated to streets, and The result is 16.2%. Given that the study area is part of the city, road buffer zones were appropriately set at the boundary to improve connectivity between adjacent regions and obtain more accurate accessibility calculation results.

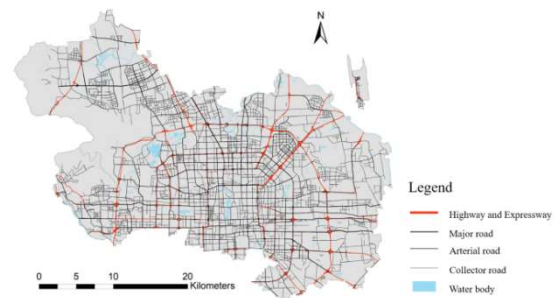


Figure 4. Road classification results and road density map

Road level	Motorway	Trunk	Primary	Secondary	Tertiary	Service	Residential/ Living street	Pedestrian/ Footway
Width(m)	50	40	30	25	20	15	10	5

Table 3. The road widths used in this study

The Worldpop population data for China, which was segmented by age and gender, was clipped according to the five districts of Beijing and projected into a unified coordinate system. The population statistical results for Dongcheng and Xicheng districts were 2.102 million people, while the seventh national population census reported a resident population of 1.815 million people in the core area of Beijing, with an error rate of 15.8%.

3.2 Accurate sample sets of UGS using high-resolution images

The high-resolution satellite imagery from Gaofen-2 conducted orthorectification and geometric correction before the multispectral and panchromatic images are fused. Currently, there are two popular fusion methods, the Gram-Schmidt fusion and the NNDiffuse fusion, which both preserve color, texture, and spectral information well. However, the NNDiffuse method

tends to produce a blue-colored bias in the fused results when there are large water bodies in the image (Figure 5). As green space samples need to be created based on the fused images, a blue bias can impede the identification of ground objects. Therefore, the Gram-Sch method is chosen.

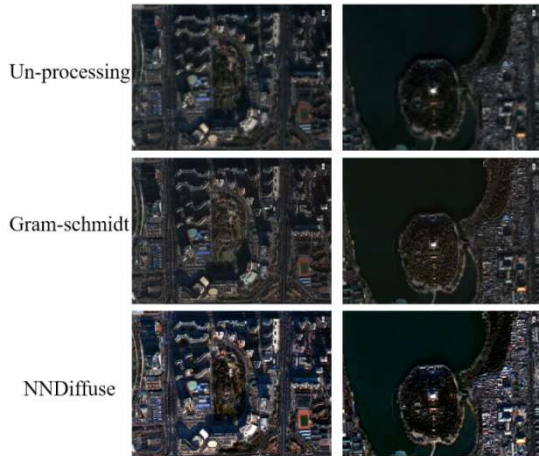


Figure 5. Comparison of the effects of different fusion methods before and after the preprocessing of GF-2 image

The fused Gaofen-2 imagery is segmented into 5120*5120 sized images, of which 48 are uniformly selected for manual visual interpretation based on the "Urban Green Space Classification Standards", with samples labeled for park green space (Figure 6, (a)) and affiliated green space (Figure 6, (b)). Both categories of urban green space in Beijing are accurately marked to improve the effectiveness of deep learning models. These 48 images can generate 768 annotated images, which can be augmented to create 3072 training samples. The model was trained for 100 epochs, with the final loss value reaching 0.0024 (Figure 7). Specifically, the recognition performance of green spaces in parks is superior to that of affiliated green spaces, as evidenced by the clearer external contours of green spaces in parks and the ability to discern roads and water bodies. However, there is a problem of missing segmentation, where small holes may appear in the middle of green spaces (Figure 8, (a)). Moreover, affiliated green spaces are susceptible to misidentification, where residential buildings may be mistakenly identified as green spaces (Figure 8, (b)).

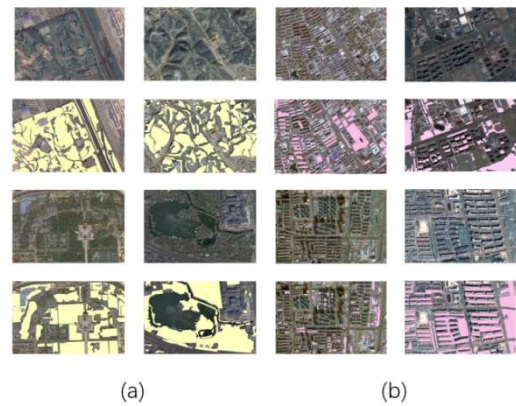


Figure 6. Urban green space sample sets

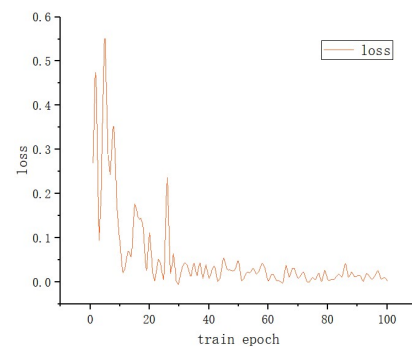


Figure 7. The U-Net Train loss(100 epochs)

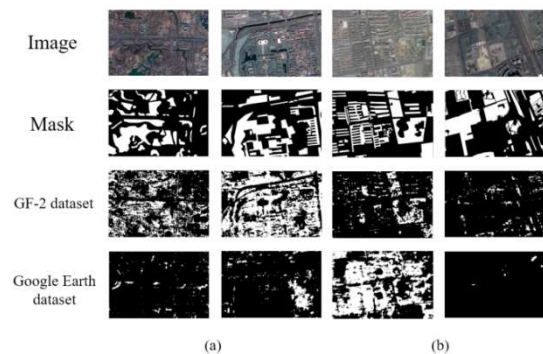


Figure 8. Training results of different data sets in U-Net model

According to the method mentioned in Section 2.2.3, the accuracy of the identified urban green spaces was validated. A total of 200 validation points were randomly selected within the study area for this purpose. The identification results were compared with the contemporaneous Google imagery and UGS-1m dataset. The obtained results are shown in Table 4 and 5.

UGS-1m	Predicted	Predicted
	Positive	Negative
Actual Positive	91	12
Actual Negative	9	88

Table 4. Confusion Matrix Comparison: our method vs UGS-1m

Google Image	Predicted Positive	Predicted Negative
Actual Positive	94	8
Actual Negative	6	92

Table 5. Confusion Matrix Comparison: our method vs Google Image

The accuracy, precision, recall, and F1 score, compared to UGS-1m and Google Image respectively, all exceed 90%. The proposed method performs better in Google Image. This indicates that the proposed method achieves a high level of performance in terms of accuracy, precision, recall, and F1 score. It demonstrates the reliability and effectiveness of the proposed method in accurately identifying and classifying images, surpassing the 90% threshold for these evaluation metrics. Such results highlight the superiority of the proposed method and demonstrate its potential for practical applications in image analysis and recognition tasks.

	UGS-1m	Google Image
Accuracy	90%	93%
Precision	91%	94%
Recall	88%	92%
F1 Score	90%	93%

Table 6. Accuracy assessment metrics

3.3 Performance of UOS identification model optimized by AOI data

The U-Net model has been trained to achieve promising results in UGS, which is part of UOS. However, using only the identification results of UGS as UOS is far from sufficient. In this study, OSM data was incorporated to refine the precise location of UGS based on the identified results. This includes segmenting the objects based on the road network and merging objects with similar semantics in spatial terms.

By aggregating the UGS identification results and utilizing urban roads to segment the UGS, the study have selected green spaces larger than 400m² as urban green space areas. The study have also fused this information with OpenStreetMap's AOI data for parks and squares. This study employs a geospatial overlay analysis technique to integrate the results of UGS recognition with AOI data, delineating overlapping areas as UOS. Furthermore, any unrecognized green open spaces are supplemented with OSM data.

3.4 The overall characteristics of UOS service range considering gender and age

In accordance with the approach outlined in Section 2.2.2, the calculation of road speed, traffic probability, and time cost was conducted. Subsequently, the roads were rasterized, with time cost used as the value of each pixel and a resolution of 10m. The areas outside of the roads were designated as pedestrian areas with a speed of 3.5 km/h. OSM water data was included as a mask, and water areas were designated as impassable. City open space accessibility was computed based on the cost of road rasterization and city open space, with the results reclassified and analyzed for service area every 2 minutes (Figure 9), followed by the calculation of the cumulative proportion of the serviced population (Figure 10, (b)).

As shown in Figure 9, most areas within the five central districts in Beijing have a city open space accessibility time of under 10 minutes. The area between the 3rd and 4th Ring Roads displays moderately accessible zones with localized clustering. In the northeast and northwest of the study area, there are areas with a 10-20 minute accessibility zone, typically in areas with lower road density. However, there are areas that are difficult to access city open spaces, including the airport in the northeast, locating nearby the western, northwestern, and eastern edges of the study area.

After resampling the spatial accessibility map using population density data stratified by gender and age, zoning statistical analysis is used to obtain the number and proportion of corresponding populations in each accessibility level (Figure 10, (a1-a8)(c1-c8)). According to Figure 10, it can be inferred that regardless of age group, the gender gap in urban open space service coverage rates is not significant. The gender ratio remains at a basic 1:1, with the largest difference in proportions being that women aged 70-75 have 5% more access to these services compared to men of the same age group. These findings indicate that in Beijing City, both children and the elderly can enjoy convenient services when using UOS.

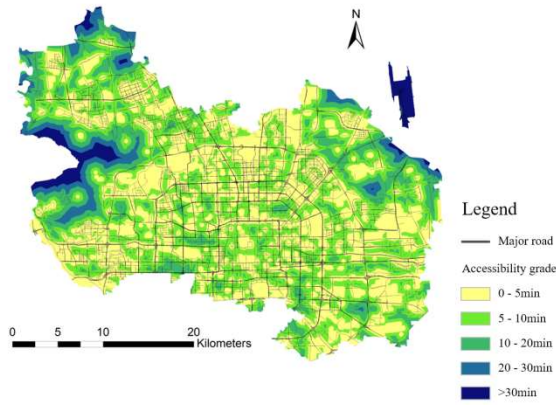


Figure 9. Service coverage analysis map and Cumulative service number chart

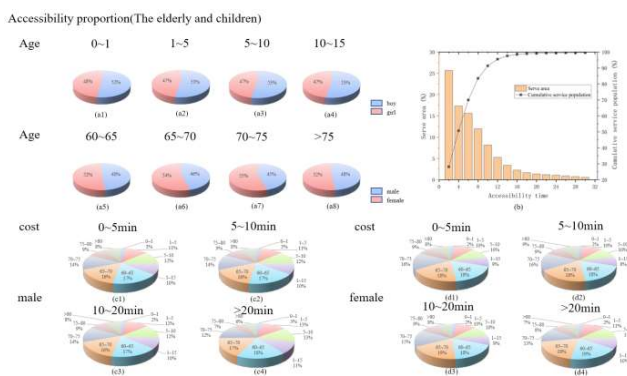


Figure 10. Calculation of the proportion of urban open space accessible to population by age and sex

4. CONCLUSIONS

This study introduces a deep learning U-Net framework that leverages earth observation advantages to extract UGS using sub-meter satellite images. This provides a more accurate approach to evaluate SDG 11.7.1 indicators and explores the accessibility of services based on gender, age, especially for the elderly and children. The use of remote sensing data with wide observation coverage and low cost at the urban level enhances the sustainable development of cities.

Due to the significant impact of data quality on research results, it is necessary to study the accurate extraction of urban built-up areas and the finer spatialization of population data in future works. Moreover, obtaining time-series data composed of multiple high-precision satellite images is needed to monitor UOS dynamics. This will enable more accurate evaluation of SDG 11.7.1 indicators, which, in turn, will facilitate the construction of inclusive, safe, resilient, and sustainable cities and human settlements.

ACKNOWLEDGEMENTS

This research was funded by the National Natural Science Foundation of China, (grant number 41930650). We are grateful to all of those with whom we have had the pleasure to work during this and other related projects.

REFERENCES

- Abascal, A., Rodriguez-Carreno, I., Vanhuyse, S., Georganos, S., Sliuzas, R., Wolff, E., Kuffer, M. 2022. Identifying degrees of deprivation from space using deep learning and morphological spatial analysis of deprived urban areas. *Computers Environment and Urban Systems*, 95, 20.
- Aguilar, R., Kuffer, M. 2020. Cloud Computation Using High-Resolution Images for Improving the SDG Indicator on Open Spaces. *Remote Sensing*, 12, 17.
- Ali, A., Fan, Y. Y. 2017. Unsupervised feature learning and automatic modulation classification using deep learning model. *Physical Communication*, 25, 75-84.
- Colglazier, W. 2015. Sustainable development agenda: 2030. *Science*, 349, 1048-1050.
- Giuliani, G., Petri, E., Interwies, E., Vysna, V., Guigoz, Y., Ray, N., Dickie, I. 2021. Modelling Accessibility to Urban Green Areas Using Open Earth Observations Data: A Novel Approach to Support the Urban SDG in Four European Cities. *Remote Sensing*, 13, 26.
- Han, L. Y., Lu, L. L., Lu, J. Y., Liu, X. T., Zhang, S. C., Luo, K., He, D., Wang, P. L., Guo, H. D., Li, Q. T. 2022. Assessing Spatiotemporal Changes of SDG Indicators at the Neighborhood Level in Guilin, China: A Geospatial Big Data Approach. *Remote Sensing*, 14, 19.
- Kavvada, A., Metternicht, G., Kerblat, F., Mudau, N., Haldorson, M., Laldaparsad, S., Friedl, L., Held, A., Chuvieco, E. 2020. Towards delivering on the sustainable development goals using earth observations. *Remote Sensing of Environment*, 247, 8.
- Liang, X., Tian, H., Li, X., Huang, J. L., Clarke, K. C., Yao, Y., Guan, Q. F., Hu, G. H. 2021. Modeling the dynamics and

- walking accessibility of urban open spaces under various policy scenarios. *Landscape and Urban Planning*, 207, 16.
- Maso, J., Serral, I., Domingo-Marimon, C., Zabala, A. 2020. Earth observations for sustainable development goals monitoring based on essential variables and driver-pressure-state-impact-response indicators. *International Journal of Digital Earth*, 13, 217-235.
- Pafi, M., Siragusa, A., Ferri, S., Halkia, M. 2016. Measuring the accessibility of urban green areas. In *A Comparison of the Green ESM With Other Datasets in Four European Cities*, Publications Office of the European Union: Luxembourg.
- Ronneberger, O., Fischer, P., Brox, T. 2015. U-Net: Convolutional Networks for Biomedical Image Segmentation. *Lecture Notes in Computer Science [Medical image computing and computer-assisted intervention, pt iii]*. 18th International Conference on Medical Image Computing and Computer-Assisted Intervention (MICCAI), Munich, GERMANY.
- Shi, Q., Liu, M. X., Marinoni, A., Liu, X. P. 2023. UGS-1m: fine-grained urban green space mapping of 31 major cities in China based on the deep learning framework. *Earth System Science Data*, 15, 555-577.
- Toger, M.; Malkinson, D.; Benenson, I.; Czamanski, D. 2016. The connectivity of Haifa urban open space network. *Environment and Planning B-Planning & Design*, 43, 848-870.
- UN-Habitat. 2018. *SDG Indicator 11.7.1 Training Module: Public Space*. United Nations Human Settlement Programme (UN-Habitat), Nairobi.
- Verde, N., Patias, P., Mallinis, G. 2022. A Cloud-Based Mapping Approach Using Deep Learning and Very-High Spatial Resolution Earth Observation Data to Facilitate the SDG 11.7.1 Indicator Computation. *Remote Sensing*, 14, 19.
- Wai, A. T. P., Nitivattananon, V., Kim, S. M. 2018. Multi-stakeholder and multi-benefit approaches for enhanced utilization of public open spaces in Mandalay city, *Myanmar: Sustainable Cities and Society*, 37, 323-335.
- WorldPop and Center for International Earth Science Information Network (CIESIN), 2018. *Global High Resolution Population Denominators Project - Funded by The Bill and Melinda Gates Foundation (OPP1134076)*. <https://dx.doi.org/10.5258/SOTON/WP00646>
- Zhu, Y. Y., Ling, G. H. T. 2022. A Systematic Review of Morphological Transformation of Urban Open Spaces: Drivers, Trends, and Methods. *Sustainability*, 14, 22.